

# Automated, Label-Free, Kinetic Neurite Outgrowth Analysis

Kinetic, label-free neurite outgrowth evaluation of live iPSC-derived neuronal cultures, enabled by a fully automated, multimodal imaging and analysis platform

## Authors

Rebecca Mongeon, PhD  
Joe Clayton, PhD  
Agilent Technologies, Inc.

## Abstract

Label-free cellular analysis provides a means to monitor and evaluate live cells over time with minimal intervention. Analysis of live neurons using label-free methods represents an important technique for high-throughput, image-based neurite outgrowth assays. Agilent BioTek automated imaging systems feature integrated environmental controls and multiplate capacities to enable a diverse range of long-term live-cell applications. This combination of automated live-cell microscopy and image analysis enabled by the Agilent BioTek Gen5 neurite outgrowth module presents a flexible, automated platform for label-free, kinetic neurite outgrowth studies. Neurite outgrowth analysis capabilities are demonstrated for multiple label-free imaging techniques through proof-of-principal investigations using an iPSC-derived neuron culture model. Automated image collection and analysis were performed in a high-density microplate format that enabled analysis of both time- and concentration-dependent changes to neuron culture outgrowth across multiple phenotypic parameters.

## Introduction

The in vitro neurite outgrowth assay is an established method for evaluating neuron structure and function across a broad range of neuroscientific studies, including neurotoxicity and neurodegeneration.<sup>1-3</sup> Recent advances in the development of neuronal culture models using induced pluripotent stem cell (iPSC)-derived neurons provide unprecedented opportunities for relevant and scalable in vitro human neuronal models for neurobiology research.<sup>4</sup> Cultured iPSC-derived neurons exhibit key cellular events involved in neurite outgrowth, providing an essential cell model for incorporation into the standardized battery of benchmarked in vitro assays for evaluating developmental neurotoxicity.<sup>5</sup> Furthermore, iPSC-derived models support personalized medicine approaches that require in vitro screening applications to predict adverse drug reactions.<sup>6</sup>

Label-free methods present an opportunity to evaluate neuronal outgrowth in live cells with minimal sample manipulation. Compared to label-free approaches, fluorescent models for live-cell analysis require significant investments in both model development and validation, given the need to demonstrate that the fluorescent markers do not interfere with the biology under investigation. In contrast, label-free methods are immediately accessible across sample types, including samples for which fluorescent modifications may be impractical. Furthermore, the cytotoxic and phototoxic effects commonly associated with fluorescent protein expression or dyes are avoided with label-free approaches.<sup>7</sup> Label-free methods, however, do not afford specificity in analysis, and so are only appropriate for investigations of relatively pure cell populations and have limited use for neurite outgrowth analysis in the context of more complex models, such as cocultures.

In this application note, we investigate neuron culture outgrowth of an iPSC-derived glutamatergic cell model using label-free imaging techniques for live-cell analysis. We detail how automation of both the image collection and analysis processes facilitates sensitive, high-throughput evaluation of neurite outgrowth while minimizing user intervention and effort. The automated kinetic imaging approach provides detailed insights into time-dependent differences between treatments that are difficult or impossible to capture through end-point evaluations. Furthermore, insights gained from kinetic live-cell studies can guide decisions around key time frames for follow-up investigations with end-point analyses.

Small-molecule modulators of neurite outgrowth were applied to iPSC-derived neuron cultures across a concentration series to investigate both time- and concentration-dependent effects on outgrowth. Multiple cellular phenotypic measurements relevant to neuron culture outgrowth, including length and branching parameters, were evaluated to demonstrate the performance of this platform for high-throughput, label-free approaches in neurite outgrowth studies.

## Experimental

### Materials

#### Chemicals

All chemicals were purchased from Sigma unless otherwise noted, including the outgrowth effectors blebbistatin (part number B0560), 6BIO (part number B1686), and triptolide (part number T3652). Staurosporine was purchased from Tocris Bioscience (part number 1285).

#### Cell culture

iCell GlutaNeurons (FUJIFILM Cellular Dynamics, Inc.; part number R1061) were cultured in BrainPhys Neuronal Medium (StemCell Technologies; part number 05790) supplemented with iCell Neural Supplement B (iCell kit component), iCell Nervous System Supplement (iCell kit component), N-2 Supplement (Gibco; part number 17502048), and laminin (Sigma; part number L2020). iCell GlutaNeuron cultures were plated on Greiner glass-bottom, 96-well microplates (Greiner; part number 655892). Microplates prepared for iCell GlutaNeuron cultures were first coated with poly-L-ornithine solution (Sigma; part number A-004-M), followed by complete media supplemented with laminin.

#### Instrumentation

The Agilent BioTek BioSpa live cell analysis system, comprised of the BioSpa 8 automated incubator and the Agilent BioTek Cytation 5 cell imaging multimode reader (in this case), was used to automate the live-cell workflows. The Cytation 5 was outfitted with a 20x phase contrast objective (part number 1320517) and the BioSpa 8 software managed the environmental conditions and imaging sessions.

## Methods

### Cell culture

Culture procedures followed manufacturer recommendations for iCell GlutaNeurons. Microplates were prepared for culture the day before plating. Plates were first coated overnight at room temperature with poly-L-ornithine solution. The following day, coated plates were rinsed five times with sterile phosphate-buffered saline (PBS) and incubated in a humidified tissue culture incubator (at 37 °C and 5% CO<sub>2</sub>) for at least one hour before plating cells with complete media.

iCell GlutaNeurons were thawed and plated following manufacturer protocol recommendations. Live cell estimations were performed with the trypan blue exclusion method. Cells were plated at a density of ~ 10,000 live cells per well. To minimize evaporative effects across the plate, regions between wells were partially filled with sterile water. To promote even cell dispersal across the well, plates were allowed to rest at room temperature for ~ 30 minutes to permit cell adhesion before transferring to the BioSpa 8 automated incubator with humidity and environmental controls set at 5% CO<sub>2</sub> and 37 °C. Imaging was started after approximately 45 minutes of equilibration within the BioSpa 8 automated incubator.

After 24 hours of initial outgrowth, the microplate was removed from the BioSpa 8 incubator, and a dilution series of outgrowth effectors were applied to cultures during a 50% media exchange. An additional 50% media exchange was performed 48 hours later (72 hours postplating) with maintenance of final drug concentrations.

### Image capture and processing

Default settings of the Gen5 neurite outgrowth module provided a starting point for soma and neurite detection, and were further optimized as shown in Table 1. Optimal values for the parameters indicated in Table 1 will vary based on experimental conditions, and users are expected to evaluate and adjust these parameters as needed.

**Table 1.** Agilent BioTek Gen5 neurite outgrowth module detection settings.

Neurite Outgrowth Analysis Settings		
Soma Detection	Phase Contrast	Brightfield
Threshold Slider Level	Neutral	Neutral
Minimum/Maximum Size	10/100	10/100
Soma Closing Size	2	1
Rolling Ball Diameter	5	10
Image Smoothing Strength	15	10
Neurites		
Detection Mode	Intensity	Intensity
Threshold Slider Level	70	80
Neurite Mask Closing Size	0	0
Rolling Ball Diameter	3	5
Image Smoothing Strength	3	3
Discard Short Neurites	10	10
Discard Short Fragments	10	10
Discard Short-Ending Branches	10	10

### Data analysis and fitting

Agilent BioTek Gen5 software was used for all data plotting and fitting, unless otherwise noted. Evaluations of average outgrowth rates were evaluated using the MeanV calculation. The maximal rate of change in outgrowth was evaluated using the MaxV calculation. Dose-response relationships were fit with four-parameter logistic curves, and Z-scores were calculated using the difference between the treatment mean and control mean expressed in multiples of the standard deviation of control. In the Gen5 software syntax, the following formula was applied in a transformation step to calculate the Z-score for outgrowth metrics:  $(X - \text{MEAN}(\text{CTL1})) / \text{SD}(\text{CTL1})$ .

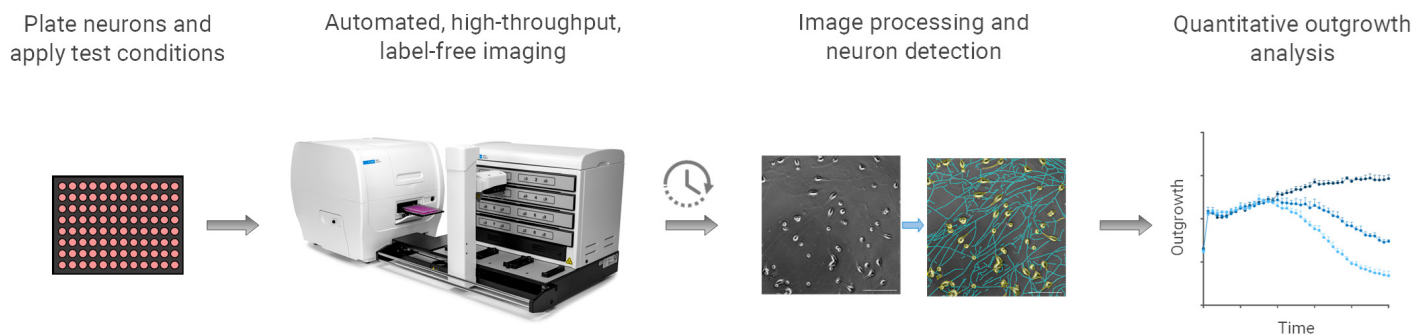


**Figure 1.** Generalized workflow for automated, label-free neurite outgrowth assays with the Agilent BioTek BioSpa 8 live cell analysis system. The system supports label-free image collection for multiday outgrowth assays for up to eight microplates. Agilent BioTek Gen5 software performs image analysis to quantify neurite outgrowth, as well as the downstream data analysis needed to evaluate kinetic responses and concentration-dependent treatment effects.

## Results and discussion

### Live-cell neurite outgrowth with the Agilent BioTek live cell analysis system

A generalized label-free kinetic neurite outgrowth assay schematic is shown in Figure 1. Cultures were plated on high-density microplates and imaged for evaluation across five days of outgrowth. The BioSpa 8 automated incubator was used to automatically deliver microplates to the Cytation 5 cell imaging multimode reader across multiday imaging sessions. Label-free images of neurons collected in phase contrast or brightfield imaging modes were automatically captured on the Cytation 5 across the plate and analyzed with the neurite outgrowth module in Gen5 software. Neuron cultures were assessed across multiple metrics of outgrowth, including total and average neurite outgrowth length. Both kinetic and dose–response analyses were performed in Gen5 software to evaluate treatment effects on outgrowth.

The BioSpa 8 automated incubator supports long-term outgrowth evaluations for up to eight microplates and is compatible across the Cytation instrument line, including the Agilent BioTek Cytation C10 confocal imaging reader. For lower-throughput (e.g., single microplate), kinetic neurite outgrowth assays, the Agilent BioTek Lionheart FX automated microscope is also compatible with the Gen5 neurite outgrowth module in both label-free and fluorescent imaging modes.

### Label-free neurite outgrowth analysis comparing phase contrast and brightfield methods

Agilent BioTek imagers support multiple modes for label-free imaging, including phase contrast and brightfield methods. Phase contrast imaging is a commonly used method to enhance the signal-to-noise (contrast) of neurons and neurite processes for label-free imaging.

Although phase contrast is typically the preferred method for label-free imaging of neurons, brightfield imaging was explored as an alternative label-free imaging method that does not require specialized objectives. iPSC-derived neuron culture outgrowth was assessed by imaging at 20x magnification in both phase contrast and brightfield imaging modes (Figure 2).

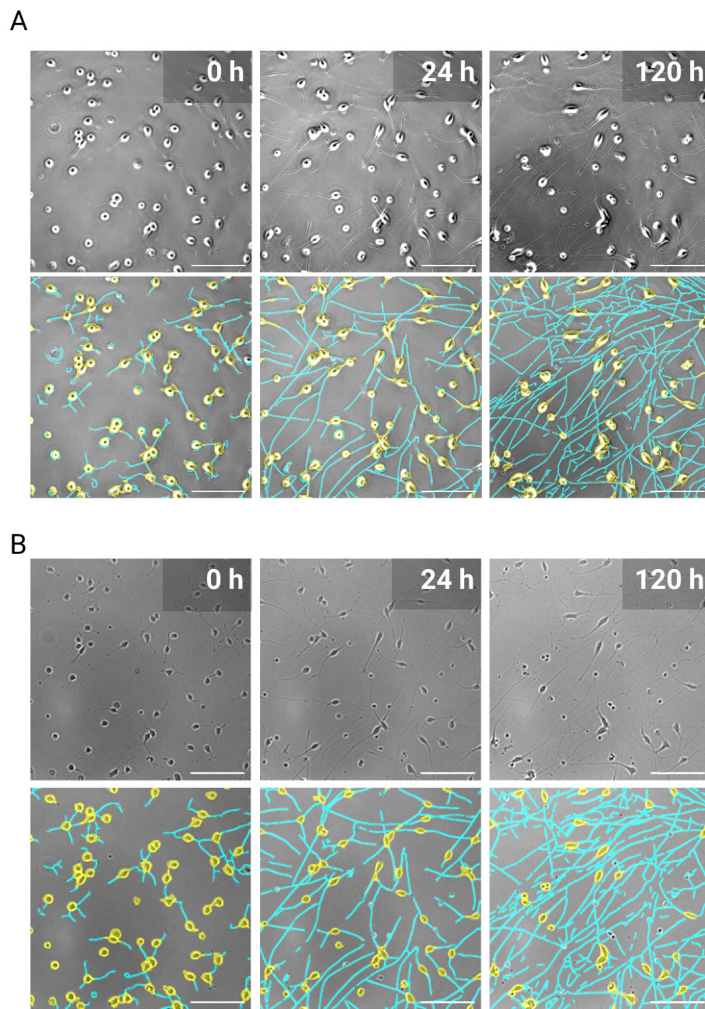
Example phase contrast images of iCell GlutaNeuron cultures at three time points are displayed in Figure 2A. Minimal outgrowth is detected in the first image taken directly following plating (Figure 2A, left panel). Neurons rapidly extend processes and a substantial increase in outgrowth is observed by 24 hours (Figure 2A, middle panel). Neurons continue to gradually increase neurite outgrowth through the five-day time course (Figure 2A, right panel). Gen5 neurite outgrowth module analysis performed on iCell GlutaNeuron cultures detected both soma and neurites in phase contrast images at each time point as depicted in the bottom panels of Figure 2A.

Example brightfield images of iCell GlutaNeurons throughout the experiment are depicted in Figure 2B, corresponding to the same field of view and time points indicated in Figure 2A. Gen5 neurite outgrowth analysis on brightfield images identified soma and neurites at each time point as depicted in the bottom panels of Figure 2B.

Neurite outgrowth was quantified over time using the Gen5 neurite outgrowth module and is presented as total neurite length over time for both phase contrast and brightfield. The mean total neurite outgrowth length for all untreated wells ( $n = 12$ ) is presented in Figure 2C for both imaging methods. Phase contrast imaging generally provided increased contrast for neurite detection, however, similar outgrowth results were quantified using both imaging methods, suggesting that brightfield imaging strategies may also be suitable for neurite outgrowth analysis with this platform. For simplicity, throughout the remainder of this application note, neurite outgrowth analysis is limited to phase contrast imaging.

## Kinetic evaluation of label-free outgrowth

To evaluate the rate of outgrowth, the per-cell average neurite length was calculated (Figure 2D) and fit using linear regression over the period of 24 to 120 hours (Figure 2D, black lines fit overlay). The average per-cell outgrowth rate over this time corresponded to  $\sim 15 \mu\text{m}/\text{day}$ . The outgrowth assay shown in Figure 2, panels A to D, was intended to capture changes in outgrowth over several days, so the imaging interval was set to collect images every three hours. However, iCell GlutaNeurons demonstrated an apparent jump in outgrowth between the initial image and the next imaging time point taken three hours later (Figure 2C and D).



To explore this initial increase, a separate experimental kinetic evaluation (Figure 2E) was performed at a higher imaging frequency to capture the time course of this early outgrowth. Images captured at 10-minute intervals confirmed that iCell GlutaNeurons exhibited a rapid and continuous increase in outgrowth over the first three hours in culture. Gen5 analysis of the average neurite outgrowth length over the first three hours in culture yielded per-cell outgrowth rates of  $\sim 500 \mu\text{m}/\text{day}$  (Figure 2F). After the initial early outgrowth period, neurons transitioned to a gradual outgrowth phase ( $15 \mu\text{m}/\text{day}$ , Figure 2D) over the next days in culture.

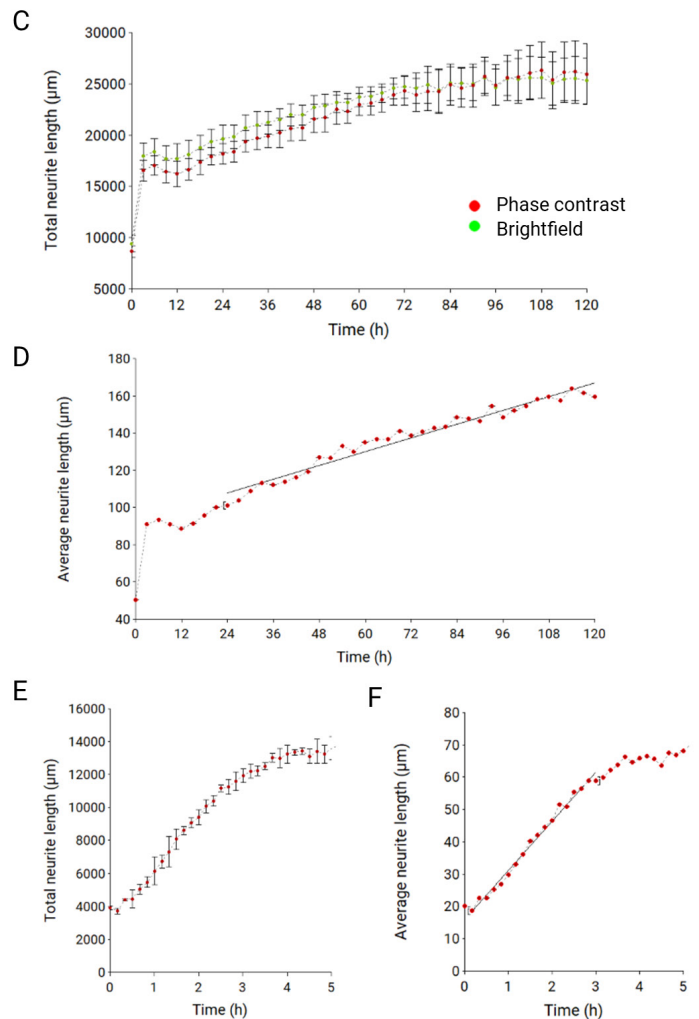


**Figure 2.** Automated image capture and kinetic outgrowth analysis. (A) Top: Phase contrast images of iPSC-derived neurons at three time points after plating as indicated. Bottom: Phase contrast images from the top row after neurite outgrowth analysis with soma (yellow) and neurite skeleton (cyan) overlay. Scale bars correspond to  $200 \mu\text{m}$ . (B) Top: Brightfield images from the same field of view as shown in panel A. Bottom: Brightfield images from the top row after neurite outgrowth analysis with soma (yellow) and neurite skeleton (cyan) overlay. Scale bars correspond to  $200 \mu\text{m}$ . (C) Total neurite length plotted over five days of outgrowth evaluated for phase contrast (red) and brightfield (green) images for all iCell GlutaNeuron control wells (including representative images shown). Data points correspond to mean of technical replicate wells ( $n = 12$ ) and standard deviation. (D) Average per-cell neurite length for all control well images. Data points (red) correspond to mean of technical replicates ( $n = 12$ ) and linear fit to mean (black line overlay) was used to determine average neurite outgrowth rate between 24 and 120 hours. (E) Total neurite outgrowth evaluated over the first 6 hours after plating by kinetic imaging every 10 minutes. Data points correspond to mean of technical replicate wells ( $n = 3$ ) and standard deviation. (F) Average per-cell neurite length evaluated over the first 3 hours in culture. Data points indicate mean of technical replicate wells ( $n = 3$ ) and linear fit to mean data (black line overlay) was used to determine average neurite outgrowth rate over the first three hours of culture.

## Kinetic evaluation of neurite outgrowth in response to drug treatment

Kinetic analysis of outgrowth for both enhancers and inhibitors of neurite outgrowth was conducted over a five-day time course. The plate view display in Figure 3 provides a high-level graphical representation of the outgrowth kinetics for each of the 96 wells throughout the experiment.

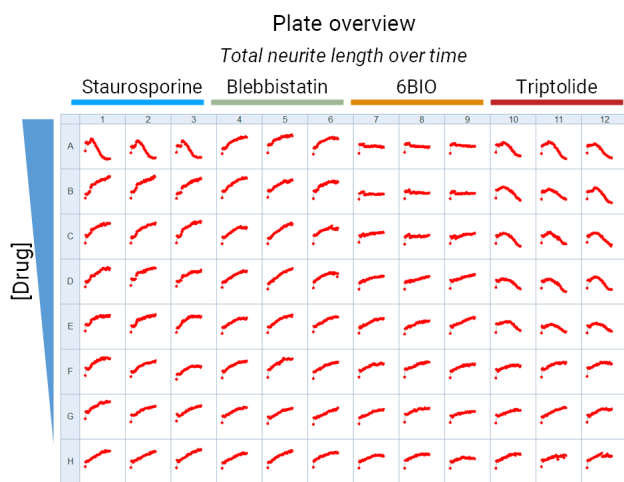


**Figure 3.** Plate layout and overview. Drugs were applied in increasing concentrations, and plots of total neurite outgrowth length over time (red) are displayed in the Agilent BioTek Gen5 software plate view for all wells.

Quantification of the total neurite length over time was plotted for the highest two drug concentrations and untreated controls (Figure 4), with representative phase contrast image and Gen5 neurite outgrowth analysis overlaid for each drug at the final time point tested.

Staurosporine is a broad-spectrum kinase inhibitor associated with multiple cellular effects including apoptosis and neurite outgrowth across multiple neuronal models.<sup>8-9</sup> A complex effect of staurosporine on iPSC-derived neuron culture can be observed in Figure 4A. The highest concentration of staurosporine tested (1  $\mu$ M) initially promoted increased neurite outgrowth over the first hours of application (Figure 4A, green trace). Initial outgrowth, however, was followed by a dramatic reduction in total neurite length, owing to generalized cell death. A rapid transition from outgrowth enhancement to cell death has previously been reported for high concentrations of staurosporine.<sup>8</sup> Application of 0.3  $\mu$ M staurosporine, however, demonstrated a rapid and sustained enhancement of neurite outgrowth without overt neurotoxicity (Figure 4A, blue trace).

Blebbistatin is a myosin II inhibitor that is thought to promote outgrowth through inhibition of retrograde actin flow.<sup>10</sup> Treatment with 10  $\mu$ M blebbistatin in this assay showed a small increase in outgrowth but was not significantly different from the control outgrowth, as evaluated by Z-score (Z-score < 2).

6BIO is an inhibitor of the glycogen synthase kinase 3 $\beta$  protein thought to be involved in multiple signaling events of neuron outgrowth.<sup>11</sup> Treatment of iCell GlutaNeurons at the highest concentration of 6BIO (10  $\mu$ M) resulted in an immediate reduction in outgrowth followed by a plateau in growth across the time frame tested (Figure 4B, green trace). Lower concentrations of 6BIO (3  $\mu$ M) resulted in similar outgrowth suppression (Figure 4B, blue trace).

Triptolide is a diterpene compound identified from a traditional Chinese medicinal herb that is under investigation for multiple anticancer effects.<sup>12</sup> Treatment with triptolide in iCell GlutaNeurons, resulted in dramatic inhibition of outgrowth over time as shown for the two highest concentrations tested (Figure 4D). It was noted, however, that the onset of outgrowth inhibition appeared to be relatively delayed compared to the other effectors of outgrowth tested here (staurosporine and 6BIO), and so comparisons of treatment onset timing were further evaluated.

### Neurite outgrowth drug-response timing

Average neurite length over time was compared for different drug responses and untreated control wells, as shown in Figure 5A. The effect of staurosporine and 6BIO on average neurite length were observed even at the first time point after drug addition. The rapid effect onset is consistent with the mechanism of action for each drug: both drugs target the signaling pathways directly involved in regulating the cytoskeletal structures required for neurite stability and extension.<sup>8,9,11</sup> By comparison, the inhibitory effect of triptolide on neurite outgrowth was relatively delayed: total neurite length remained similar to control values up to ~ 24 hours after triptolide addition. After ~ 24 hours, neurite length gradually decreased through the rest of the experimental time frame. After 72 hours of exposure (corresponding to the 96-hour image time point) triptolide had inhibited average neurite length to a greater extent than treatment with 6BIO.

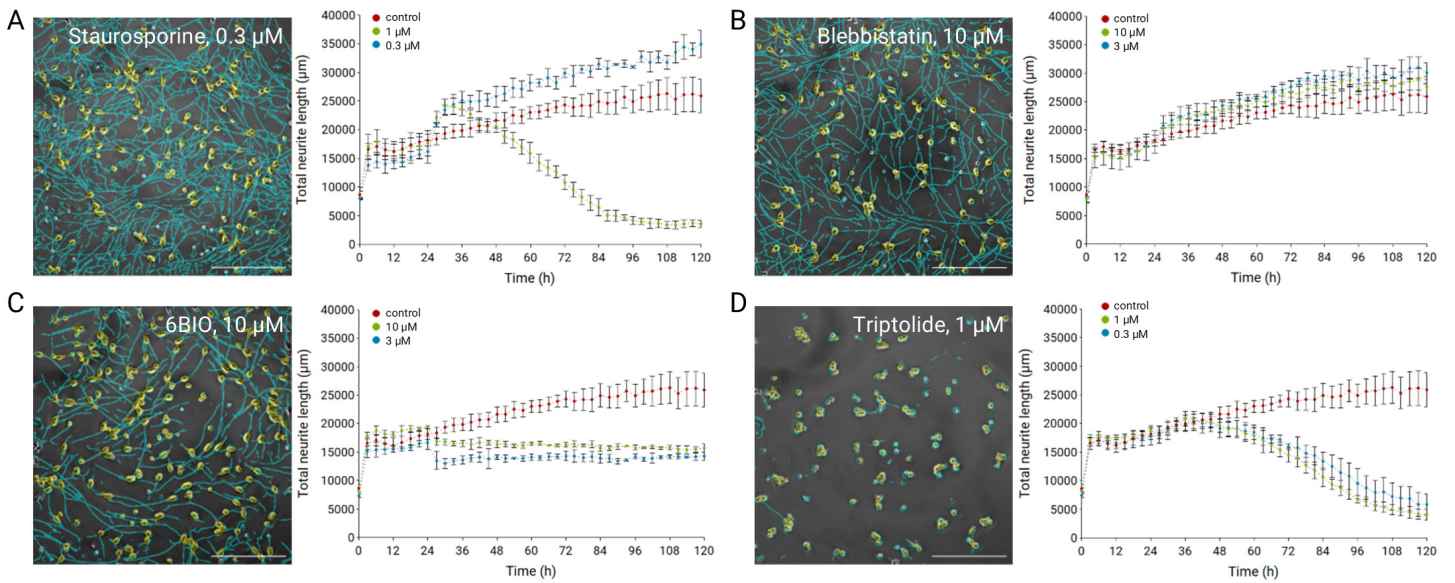


**Figure 4.** Kinetic responses of iPSC-derived neurons to outgrowth enhancers and inhibitors. (A to D) Example phase contrast image with soma (yellow) and neurite (cyan) detection overlays for neurons treated with small-molecule drugs as indicated. Image corresponds to the final kinetic time point (120 hours). The Agilent BioTek Gen5 software plot for total neurite length over time for highest (green) and second highest (blue) drug test concentration and control (red). Data points indicate mean and standard deviation of technical well replicates.

To quantify response onset, Gen5 software was used to evaluate the time point corresponding to the maximum rate of change in neurite length for each condition. The maximum rate of change was calculated over a 9-hour time window (three imaging data points). The maximum rate evaluation yielded an average posttreatment response timing that corresponded to 3 hours for staurosporine, 2 hours for 6BIO, and 46 hours for triptolide.

In addition to neurite length, the average branch counts were visualized over time for the same treatment conditions (Figure 5B). A similar response profile for average neurite branches was observed across each drug treatment when compared to average neurite length. The covariation of these two distinct morphological parameters is consistent with previous observations that treatments altering neurite length often produce a similar effect on branching-related metrics.<sup>8</sup>

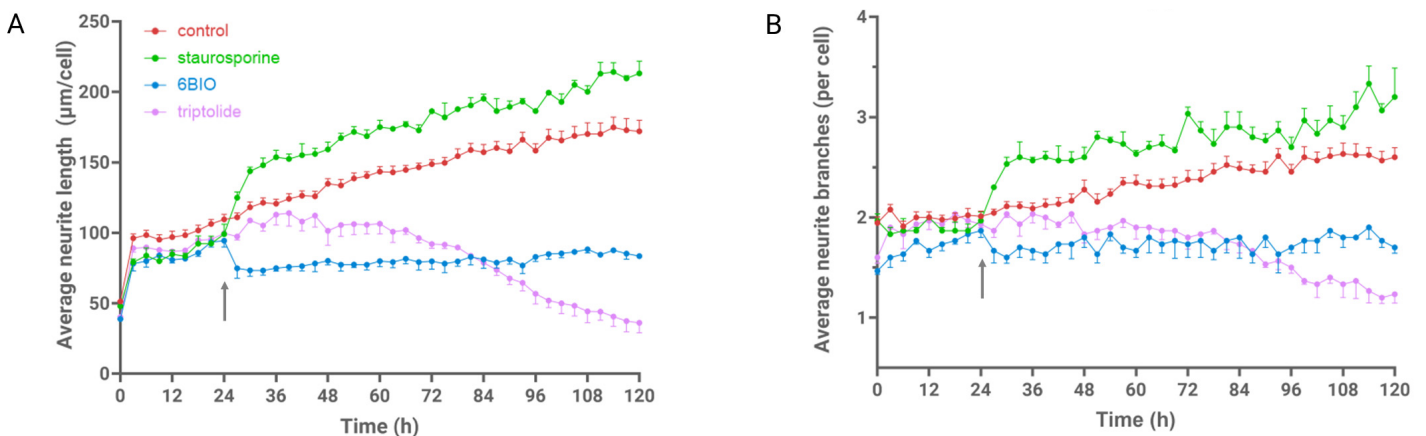


**Figure 5.** Treatment response timing comparison. (A) Average neurite length per cell over time for treatments as indicated (Prism GraphPad visualization). Data points represent mean and standard error of technical replicates ( $n = 3$ ) for each condition. Grey arrow indicates drug addition time. (B) Average neurite branches over time for the same treatments in panel A (Prism GraphPad visualization). Data points represent mean and standard error of technical replicates ( $n = 3$ ) for each condition. Grey arrow indicates drug addition time.

### Neurite outgrowth effector dose–response analysis

Drug effects on neurite outgrowth were also evaluated for concentration-dependent effects through dose–response analysis across multiple outgrowth metrics (Figure 6). For each metric, the average value over the final 12 hours of the kinetic imaging session was calculated in Gen5 software and used to generate the dose–response curves. This timeframe was chosen to represent the final treatment effect for analysis purposes. However, the region of the kinetic dataset chosen for analysis is highly customizable in Gen5 software, and supports both mean and integral (area-under-the-curve) evaluations.

Figure 6A displays the Gen5 dose–response analysis for total neurite length. Fitting provided  $EC_{50}/IC_{50}$  estimates for staurosporine (0.034  $\mu\text{M}$ ), 6BIO (0.86  $\mu\text{M}$ ), and triptolide (0.0078  $\mu\text{M}$ ). As previously noted for staurosporine<sup>8</sup> and indicated in Figure 4A, the total neurite length increased with treatment concentration until the highest concentration tested, where outgrowth was suddenly reduced, owing to cell death. Accordingly, the highest concentration was not included for fitting purposes in order to evaluate the remaining data (open circles, Figure 6A). As shown in Figure 4B, blebbistatin did not demonstrate a significant response up to the 10  $\mu\text{M}$  concentration tested here.

Dose–response analysis was also performed for branching-related neurite outgrowth metrics, as shown in Figure 6, panels B and C. Overall, treatments that decreased total neurite length were also associated with decreases in both the average number of branches per cell (Figure 6B) as well as the average neurite count per cell (Figure 6C). Fits of the average neurite branches curves in Figure 6B provided  $EC_{50}/IC_{50}$  estimates for 6BIO (0.359  $\mu\text{M}$ ) and triptolide (0.0039  $\mu\text{M}$ ), but not for staurosporine, as the response did not saturate and conform to a four-parameter fit. Significant changes in neurite counts per cell were observed only for the inhibitors in Figure 6C and corresponded to  $IC_{50}$  estimations for 6BIO (3.1  $\mu\text{M}$ ) and triptolide (0.004  $\mu\text{M}$ ).

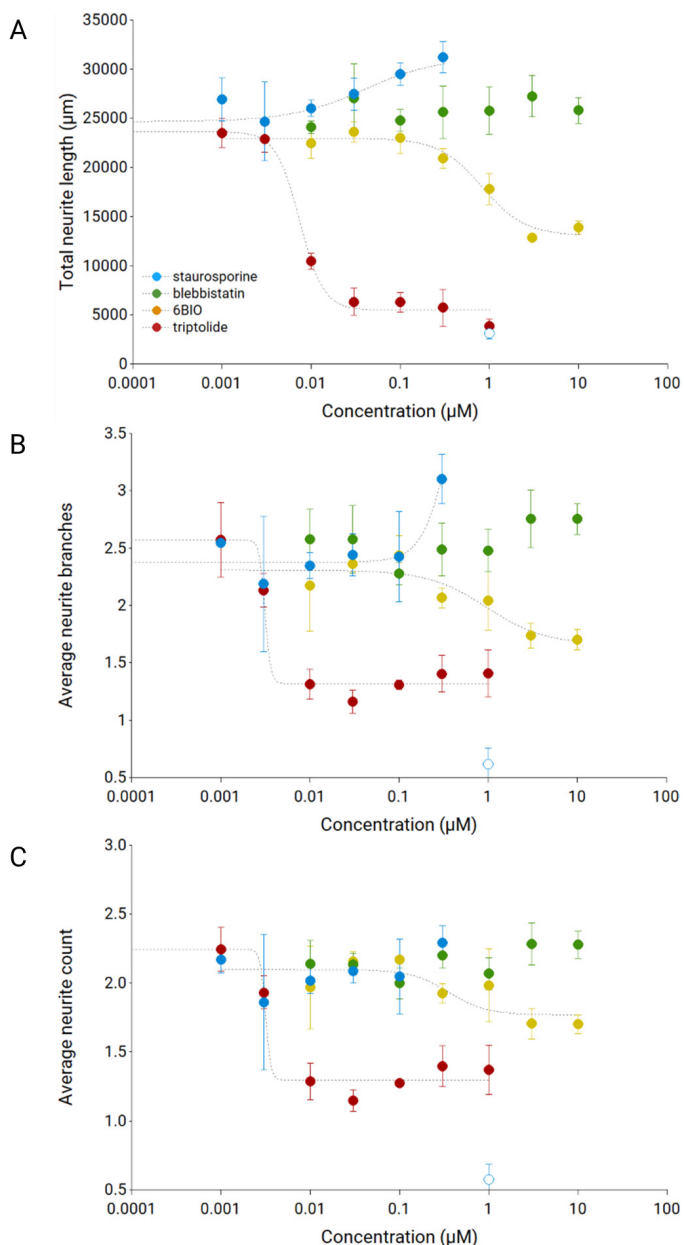


**Figure 6.** Dose–response evaluation from label-free neurite outgrowth analysis over the final 12 hours of kinetic imaging. (A) Dose–response curves for total neurite length. Data points correspond to mean and standard deviation for technical replicates ( $n = 3$ ) and corresponding four-parameter fits (dashed lines). (B) Dose–response curves for average neurite branches per cell. Data points correspond to mean and standard deviation for technical replicates ( $n = 3$ ) corresponding four-parameter fits (dashed lines). (C) Dose–response curves for average neurite count per cell. Data points correspond to mean and standard deviation for technical replicates ( $n = 3$ ) and corresponding four-parameter fits (dashed lines).



## Conclusion

Label-free imaging enables kinetic investigations in neuron culture while also avoiding the phototoxic and cytotoxic effects of fluorescence-based approaches. The Agilent BioTek BioSpa live cell imaging system for label-free neurite outgrowth assays enables high-throughput investigations with benchtop accessibility. The approach presented in this application note demonstrates quantitative kinetic neurite outgrowth analysis using multiple modes of label-free imaging techniques. Both phase contrast and brightfield transmitted light images captured on the Agilent BioTek Cytation 5 cell imaging multimode reader enabled sensitive, kinetic analysis of culture outgrowth over time. Other Cytation models, as well as the Agilent BioTek Lionheart FX automated microscope, are expected to generate comparable results. iPSC-derived neuron cultures were maintained throughout the five-day growth period by the Agilent BioTek BioSpa 8 automated incubator which maintained environmental conditions and delivered samples to the integrated imaging system. This automated robotic incubator system can maintain up to eight microplates simultaneously, increasing throughput for long-term image-based studies.

Agilent BioTek Gen5 software automated both image acquisition and analysis through a single interface. Image-processing steps, such as kinetic image alignment, were automatically handled before analysis. The Agilent BioTek Gen5 neurite outgrowth module automatically detected and analyzed both neuron soma (cell bodies) and neurite processes to provide multiple phenotypic parameters relevant for culture outgrowth analysis. Kinetic analysis of neurite outgrowth metrics, such as outgrowth length, was evaluated to determine average outgrowth rates, as well as maximum rate of change to quantify drug-response timing. In addition to time-dependent analysis, dose–response analysis capabilities provided  $EC_{50}/IC_{50}$  quantification of neurite outgrowth parameters to evaluate concentration-dependent treatment effects.

Label-free imaging and analysis capabilities on the Agilent BioTek live cell analysis system complement the imager's multimodal, fluorescence-based approaches to provide a flexible solution for a spectrum of image-based analyses methods. The combination of automated live-cell and end-point analysis provides a single-instrument solution enabling high-throughput studies across time scales and imaging modes.

## References

1. Ryan, K.R.; Sirenko, O.; Parham, F.; Hsieh, J.H.; Cromwell, E.F.; Tice, R.R.; Behl, M. Neurite Outgrowth in Human Induced Pluripotent Stem Cell-Derived Neurons as a High-Throughput Screen for Developmental Neurotoxicity or Neurotoxicity. *NeuroToxicology* **2016**, *53*, 271-281. <https://doi.org/10.1016/j.neuro.2016.02.003>
2. Al-Ali, H.; Beckerman, S.; Bixby, J.L., Lemmon, V.P. In Vitro Models of Axon Regeneration. *Exp Neurol* **2017**, *287*, 423-434. <https://doi.org/10.1016/j.expneurol.2016.01.020>
3. Logan, S.; Arzua, T.; Canfield, S.G.; Seminary, E.R.; Silson, S.L.; Ebert, A.D.; Bai, X. Studying Human Neurological Disorders Using Induced Pluripotent Stem Cells: From 2D Monolayer to 3D Organoid and Blood Brain Barrier Models. *Compr Physiol* **2019**, *9*, 565-611. <https://doi.org/10.1002/cphy.c180025>
4. Farkhondeh, A.; Li, R.; Gorshkov, K.; Chen, K.G.; Might, M.; Rodems, S.; Lo, D.C.; Zheng, W. Induced Pluripotent Stem Cells for Neural Drug Discovery. *Drug Discovery Today* **2019**, *24*, 992-999. <https://doi.org/10.1016/j.drudis.2019.01.007>
5. Blum, J; Masjosthusmann, S.; Bartmann, K.; Bendt, F.; Dolde, X.; Dönmez, A.; Förster, N.; Holzer, A-K.; Hübenthal, U.; Keßel, H.E.; Kilic, S.; Klose, J.; Pahl, M.; Stürzl, L-C.; Mangas, I.; Terron, A.; Crofton, K.M.; Scholze, M.; Mosig, A.; Leist, M.; Fritsche, E. Establishment of a Human Cell-Based In Vitro Battery to Assess Developmental Neurotoxicity Hazard of Chemicals. *Chemosphere* **2023**, *311*, 137035. <https://doi.org/10.1016/j.chemosphere.2022.137035>
6. Rispoli, P.; Piovesan, T.S.; Decorti, G.; Stocco, G.; Lucafo, M. iPSCs as a Groundbreaking Tool for the Study of Adverse Drug Reactions: A New Avenue for Personalized Therapy. *WIREs Mech Dis* **2024**, *16*, e1630. <https://doi.org/10.1002/wsbm.1630>
7. Laissue, P.P.; Alghamdi, R.A.; Tomancak, P.; Reynaud, E.G.; Shroff, H.; Assessing Phototoxicity in Live Fluorescence Imaging. *Nature Methods* **2017**, *14*, 657-661. <https://doi.org/10.1038/nmeth.4344>
8. Sherman, S.P.; Bang, A.G. High-Throughput Screen for Compounds That Modulate Neurite Growth of Human Induced Pluripotent Stem Cell-Derived Neurons. *Dis Model Mech* **2018**, *11*, dmm031906. <https://doi.org/10.1242/dmm.031906>

9. Hashimoto, S.; Hagino, A. Staurosporine-Induced Neurite Outgrowth in PC12h Cells. *Exp Cell Res* **1989**, *184*, 351-9. [https://doi.org/10.1016/0014-4827\(89\)90334-0](https://doi.org/10.1016/0014-4827(89)90334-0)
10. Costa, A.R.; Sousa, M.M. Non-Muscle Myosin II in Axonal Cell Biology: From the Growth Cone to the Axon Initial Segment. *Cells* **2020**, *9*, 1961. <https://doi.org/10.3390/cells9091961>
11. Song, Z.; Han, X.; Zou, H.; Zhang, B.; Ding, Y.; Xu, X.; Zeng, J.; Liu, J.; Gong, A. PTEN-GSK3 $\beta$ -MOB1 Axis Controls Neurite Outgrowth In Vitro and In Vivo. *Cell Mol Life Sci* **2018**, *75*, 4445-4464. <https://doi.org/10.1007/s00018-018-2890-0>
12. Noel, P.; Von Hoff, D.D.; Saluja, A.K.; Velagapudi, M.; Borazanci, E.; Han, H. Triptolide and its Derivatives as Cancer Therapies. *Trends Pharmacol Sci* **2019**, *40*, 327-341. <https://doi.org/10.1016/j.tips.2019.03.002>
13. Wang, Y.; Xu, Y.; Liu, Q.; Zhang, Y.; Gao, Z.; Yin, M.; Jiang, N.; Cao, G.; Yu, B.; Cao, Z.; Kou, J. Myosin IIA-Related Actomyosin Contractility Mediates Oxidative Stress-Induced Neuronal Apoptosis. *Front Mol Neurosci* **2017**, *10*, 75. <https://doi.org/10.3389/fnmol.2017.00075>

[www.agilent.com/lifesciences/biotek](http://www.agilent.com/lifesciences/biotek)

For Research Use Only. Not for use in diagnostics procedures.

RA45471.5722569444

This information is subject to change without notice.

© Agilent Technologies, Inc. 2024  
Published in the USA, June 18, 2024  
5994-7556EN

